Optimizing the acceleration and resolution of fat image-navigators (3D FatNavs) for high-resolution motion-correction at 7T

Daniel Gallichan[1], José P Marques[1,2]
[1]*CIBM, EPFL Lausanne, Switzerland,*
[2]*Donders Center for Cognitive Neuroimaging, Radboud University, The Netherlands*

Abstract

Purpose

To investigate the effect of spatial resolution and parallel imaging acceleration factor on the quality of the motion-estimates derived from image-navigators with a 3D gradient-recalled echo (GRE) acquisition with fat-excitation (3D FatNavs) for neuroimaging at 7T.

Methods

6 healthy subjects were scanned for 10 minutes, during which time repeated GRE volumes were acquired during small movements – alternating between fat and water excitations (WaterNavs) - allowing retrospective decimation of the data to simulate a variety of combinations of image-resolution and acceleration factor. Bias and error in the motion-estimates were then compared across navigator parameters.

Results

The 2mm, 4×4 accelerated data (TR_{volume}=1.2s) provided motion estimates almost indistinguishable from those from the full original acquisition (2mm, 2×2, TR_{volume}=5.2s). For faster navigators it was found that good accuracy and precision were achievable with TR_{volume}=144 ms, using a lower spatial resolution (4mm, 6×6 acceleration) to avoid the bias observed at exceptionally high acceleration factors (8×8 or higher). Parameter-estimates from WaterNavs and FatNavs showed close agreement with FatNavs demonstrating better performance at exceptionally high acceleration factors.

Conclusion

Data are provided to help guide parameter choice for 3D FatNavs when a compromise must be reached between the quality of the motion-estimates and the available scan time.

Introduction

With the increasing availability of ultra-high magnetic field (≥7T) MR scanners, there is a continued interest in pushing the limits of the spatial resolution that can be acquired. Images at the very highest resolutions will inevitably require extended scan times – increasing the likelihood that the image quality will be detrimentally affected by artifacts associated with motion of the subject during the scan. There have been several recent examples of effective motion-correction achieved through real-time update of the scanner coordinates based on motion estimates obtained from external tracking devices, e.g. (1–5), but all these methods have the problem of needing to affix a marker (or markers) to the subject's head, limiting their suitability for routine use. Motion information can also be estimated from additional MR acquisitions interleaved with the main sequence, referred to as motion-navigators. There are also many examples of such navigator-based methods, e.g. (6–9), but only one of these has also been demonstrated to be effective for small involuntary motion in very high resolution imaging. Using a 3D echo-planar imaging readout as the motion-navigator, Tisdall et al were able to perform motion-correction during a 138-minute scan at 350 μm isotropic resolution at 3T (10), but it is not clear if this could be applied at ultra-high magnetic field strengths due to increased prevalence of image distortions and signal dropout. Retrospective motion-correction techniques, where motion is estimated either from the data itself, or from interleaved navigator data, have also been shown to be able to correct for motion, e.g. (11–13), but these methods were also primarily tested and demonstrated for large deliberate motion of the volunteers.

We recently demonstrated that the quality of high-resolution structural imaging at 7T can be effectively improved by interleaving rapidly acquired 3-dimensional fat image-navigators (3D FatNavs) (14) within the sequence dead-time in order to track, and retrospectively correct for, the microscopic involuntary head-motion which is inevitable during an extended scan time – even for young healthy volunteers who are accustomed to the scanner environment. For the data presented in ref. (14) the 3D FatNav consisted of a 3D gradient-recalled echo (GRE) with binomial RF pulses to excite only the fat frequency at 2mm isotropic resolution and with 4×4 generalized autocalibrating partially parallel acquisitions (GRAPPA) acceleration (15). These parameters were chosen as an empirical compromise between voxel resolution and parallel imaging acceleration factors in order to fit in the available dead-time (around 1-2 s depending on the sequence and the chosen parameters). A fat excitation was used for 2 main reasons: Firstly, the fat excitation results in a sparse image which can be exploited to achieve high parallel imaging accelerations; and secondly the fat signal is rarely of interest for neurological applications, and there will be minimal effect of the presence of the navigator on the magnetization of water spins. In the present work we seek to systematically compare the effectiveness of 3D FatNavs at a range of voxel resolutions and acceleration factors, thereby aiding in the

selection of the best parameter choice – which becomes especially relevant for integration into the large number of pulse sequences with reduced, or without, 'dead-time' - where the navigator scans will unavoidably lead to a longer overall scan duration. It is clear that the accuracy and precision of the motion-estimates will affect the quality of the motion-corrected image – and previous work suggests that the accuracy of the tracking estimates should be kept to a fraction of the voxel size in order to avoid introducing additional artefacts (16).

Methods

All imaging was performed on a 7T head-only MR system (Siemens Healthcare, Erlangen, Germany) fitted with a 32-channel RF coil array, housed within a birdcage transmit coil (Nova Medical Inc., Wilmington, MA). All volunteers were healthy adults who gave written informed consent prior to the imaging in accordance with the local review board.

Experiment 1 – Comparison of estimated motion-parameters at different navigator resolution and acceleration

6 volunteers (age 19-35) were each scanned for a period of approximately 10 minutes, during which time repeated 3D-GRE volumes were acquired – with the frequency of the binomial excitation RF pulse alternating between being on-resonance for water (WaterNavs) or on-resonance for fat (FatNavs). Each volume had the same imaging parameters: 2 mm isotropic resolution, 88×128×128 matrix, TE/TR = 1.35/3.0 ms, bandwidth = 1950 Hz/pixel, flip angle = 5°, GRAPPA acceleration 2×2 = 4 (with integrated 16×16 calibration lines), ¾ partial Fourier undersampling (with zero-filling) in both phase-encoding directions, TR_{volume} = 5.2 s. All subjects were instructed to remain still during the scan, but in order to induce small movements during the short scan which approximately correspond to the range of movements expected during a longer scan an air-cushion was placed under the subject's head. The air-cushion was connected to a programmable syringe pump in the scanner control room using a long thin tube, via the waveguide. This pump was used to slowly deflate the airbag by 60 ml during approximately minutes 3 to 6, and then to reflate approximately from minutes 6 to 9. The precise timing and amplitude of the motion was not important, but we used this setup to reproduce slow 'drift' motion which is often observed in healthy subjects during extended scans.

Raw data were retrospectively decimated in order to simulate acquisitions at various spatial resolutions and GRAPPA acceleration factors. In total 17 different combinations were tested, corresponding to navigator acquisitions which would take between 140 ms and 1220 ms – with combinations of resolution/acceleration deliberately chosen to create 4 sets of navigators with approximately equivalent effective acquisition time. The GRAPPA calibration data (GRAPPA kernel 2×2) for the decimated reconstructions were taken from a separate fully-sampled acquisition (TR_{volume} = 32 s) with matched RF excitation frequency, as using integrated calibration data would not allow such high effective acceleration.

For each set of navigator parameters, reconstructed images were co-registered using a least-squares cost-function with the *realign* tool in SPM (*Statistical Parametric Mapping, version 8)* using the highest 'quality' setting (1.0), 3 mm full-width half maximum Gaussian smoothing prior to realignment, degree 2 B-spline interpolation and image samples separated by 2 mm. The 6 estimated motion parameters at each time point could then be compared to the 'true' motion – taken as the motion parameters obtained from the original 2 mm, 2×2 accelerated data for water or fat respectively.

As our MR scanner is fitted with a head-only gradient set with a relatively small region of high spatial linearity of the encoding fields we also performed unwarping using *gradunwarp* software (https://github.com/ksubramz/gradunwarp) of each of the navigator images prior to their co-registration, making use of a look-up table provided by the scanner manufacturer consisting of spherical harmonic terms describing the encoding fields. Separate co-registration of the navigators was performed both before and after the unwarping to observe its influence on the estimated motion parameters.

To compare the quality of motion-estimates between navigator parameters we calculated the 'bias', which we defined as "1 – {*slope of the linear regression of estimated motion parameters vs 'reference' motion}*", and the root mean-square (RMS) of the residuals to this regression. Translations and rotations were treated separately in the calculation of these metrics to allow investigation into potential differences in sensitivity to different kinds of motion. The 'reference' motion in each case was taken as the estimated motion parameters from the highest quality estimate available (2 mm, 2×2 acceleration) for the same excitation frequency (either on resonance for water or for fat). When comparing motion estimates with WaterNavs vs FatNavs, the estimates from WaterNavs were taken as 'reference' motion. When comparing motion estimates before and after unwarping for gradient non-linearities, the estimates from before unwarping were taken as 'reference' motion (for calculation of the metrics only, this has no effect on which parameters are the best estimates to use for motion correction – see Discussion).

The bias and the RMS residuals for translations and rotations were also combined into a single error metric for each WaterNav and FatNav parameter combination, which we defined as "$(rotation\ bias)_{F/W}$/min*(all rotation bias) +* $(translation\ bias)_{F/W}$*/min(all translation bias) + (RMS rotation residuals)*$_{F/W}$/min*(all RMS rotation residuals) + (RMS translation residuals)*$_{F/W}$/min*(all RMS translation residuals)".* This combined metric is necessarily somewhat arbitrary due to the different nature of the units involved (translations and rotations, bias and residuals) so by normalising each by its minimum value for all parameters tested we attempt to give each of these approximately equal importance.

To allow a more direct comparison of the motion estimates from FatNavs with those from WaterNavs, the motion estimates from the original 2 mm, 2×2 accelerated FatNavs

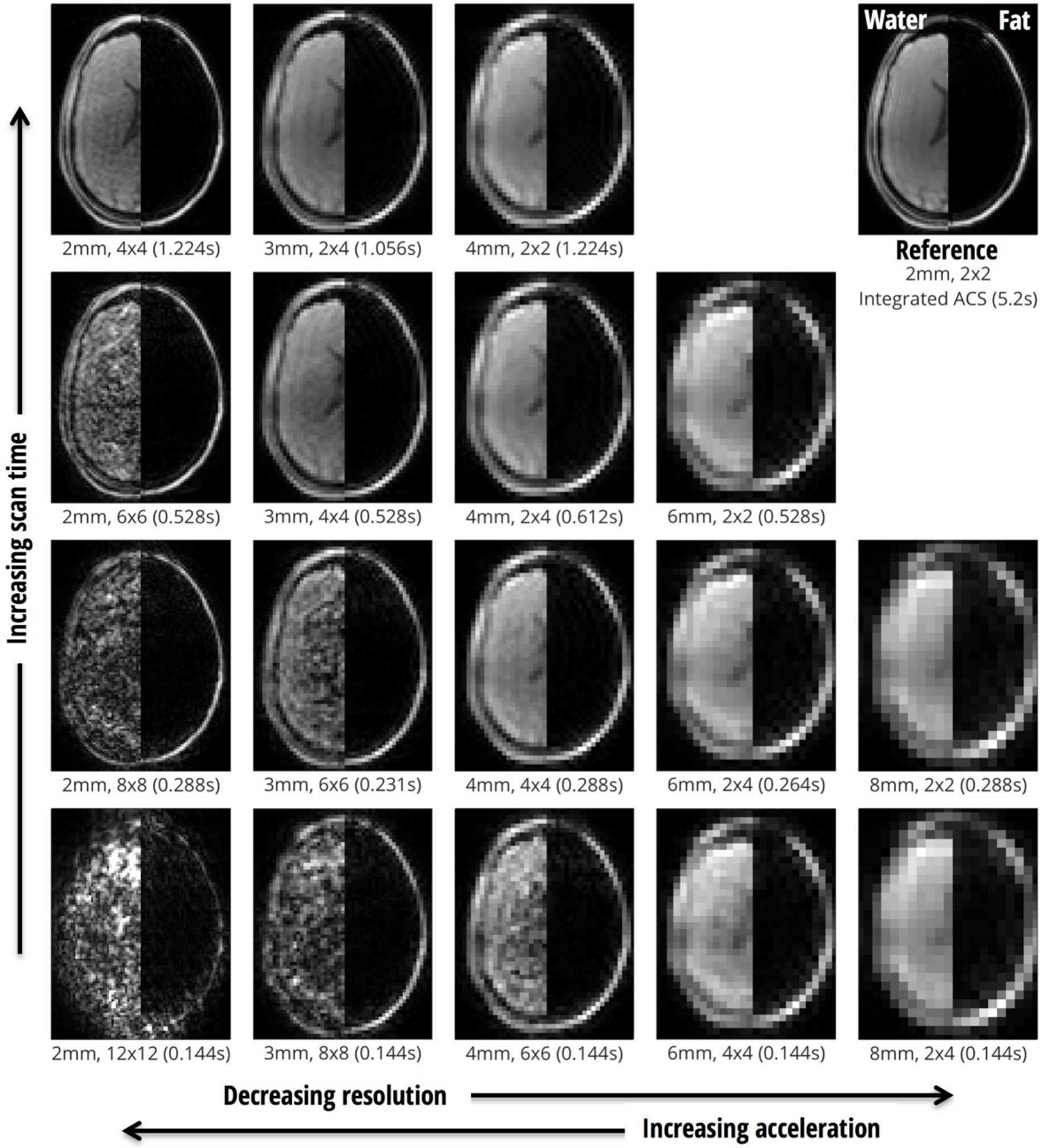

Figure 1: A single slice from the full 3D dataset of a single volume from a representative subject demonstrating the image quality for water-excitation (left side of each image) and fat-excitation (right side of each image) when reconstructed to simulate various spatial resolutions and acceleration factors. The parameters have been grouped so that each row of this figure corresponds to a navigator acquisition which would have approximately the same acquisition time per navigator (times are shown in brackets).

were interpolated to match the timing of the interleaved WaterNavs.

Experiment 2 – Quality of motion-correction using different 3D FatNav resolutions

A single subject was scanned using a 600 µm isotropic resolution MP2RAGE (*Magnetization Prepared 2 Rapid Acquisition Gradient Echoes* (17)) acquisition with a 320×320×256 matrix size, FoV 192×192×144 mm, ¾ partial Fourier undersampling in both phase-encoding directions, $TE/TI_1/TI_2/TR = 3.68/800/2700/6000$ ms, bandwidth = 240 Hz/pixel, flip angle during read-out train (TI_1/TI_2) = 7°/5°, readout direction foot/head, phase-encoding direction anterior/posterior. A GRAPPA acceleration factor of 3 was used in the first phase-encoding direction (32 reference lines) resulting in a total scan time of 10 min 8 s. A 3D FatNav volume was acquired during the dead-time of each TR after the readout-train of the second inversion time, before the next inversion pulse. The parameters for the 3D FatNav were matched to those from our previous work (14): 2 mm isotropic resolution, 4×4 = 16 GRAPPA acceleration, matrix size = 88×128×128, TE/TR = 1.35/3.0 ms, bandwidth = 1950 Hz/pixel, flip angle = 7°, readout direction foot/head, ¾ partial Fourier undersampling in both phase-encoding directions (with zero-filling). GRAPPA calibration data for the 3D FatNav was acquired by an additional prescan of 20×32 lines in 2.3 s.

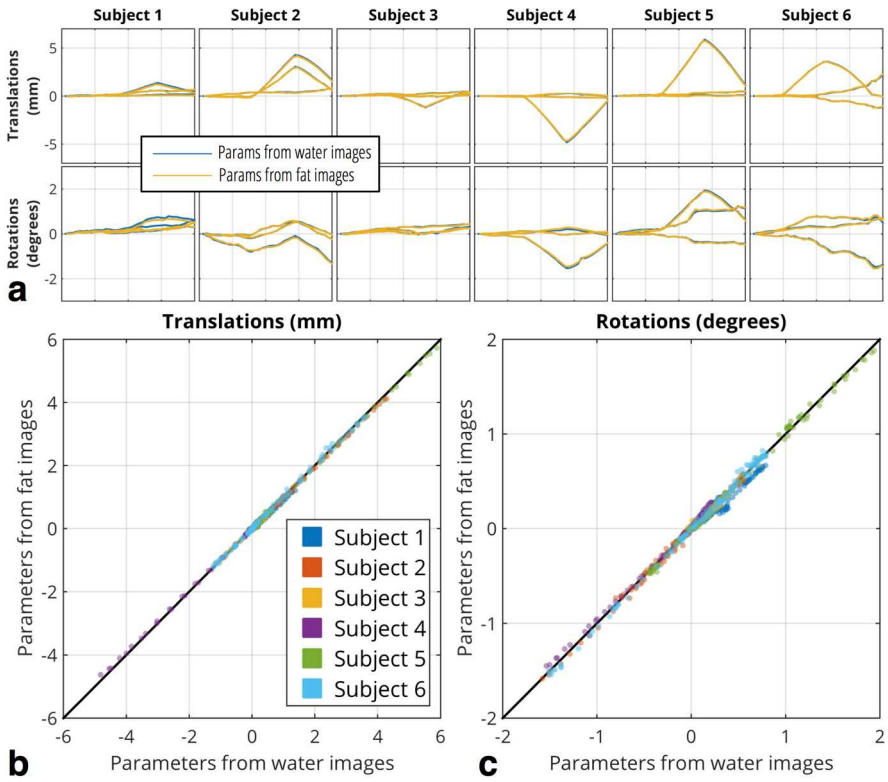

Figure 2: (a) Estimated motion parameters for all 6 subjects from the original 2 mm, 2×2 accelerated GRE navigators for the 10-minute acquisition, during which an airbag placed under the subject's head was slowly deflated and then reflated. Motion-estimates are shown derived from both water-excitation and fat-excitation data. Direct comparison of parameter estimates from each subject are also shown for (b) translations and (c) rotations – where estimates from the fat-excitation data have been temporally interpolated to match the timing of the water-excitation data.

During this scan the subject was instructed to remain as still as possible for approximately the first 3 minutes, then to initiate a series of small, slow movements in different directions for the rest of the 10 minutes. Motion-parameters were estimated from the reconstructed 3D FatNavs in the same manner as described in Experiment 1 and raw data from the host sequence were motion-corrected directly in k-space using a 3D Non-Uniform Fast-Fourier Transform algorithm (18). It should be noted that in our previous work we had not attempted to motion-correct data where the host-sequence itself was accelerated with parallel imaging. In this work we achieved this by applying the GRAPPA reconstruction to non-motion-corrected data in the conventional fashion in order to create fully-sampled non-corrected data. The 6 motion parameters for each TR were then interpolated to give pseudo-motion parameters for the k-space lines which were not acquired, but estimated via parallel imaging.

To allow comparison of the quality of image reconstruction for different resolutions of the 3D FatNav, the data from the 3D FatNavs were retrospectively downsampled to resolutions of 3, 4, 6 and 8 mm. The full pipeline of motion-estimation and retrospective motion-correction was then performed for each 3D FatNav resolution. As the 3D FatNav data were acquired at 4×4 acceleration in order to fit in the available dead-time, there was not sufficiently flexibility to also allow variation of the acceleration factors used in this experiment.

Results

Experiment 1 – Comparison of estimated motion-parameters at different navigator resolution and acceleration

The image quality of the reconstructed GRE volumes after retrospective data decimation to correspond to various spatial resolutions and acceleration factors can be observed in Fig. 1, where a single axial slice out of the full 3D volume is shown for a representative subject. The left side of each image shows the WaterNavs, and the right side shows the FatNavs. The parameter sets have been grouped such that the navigator represented in each row would take approximately the same amount of time to acquire a single navigator volume. In agreement with previous reports (14,19), the sparsity of the fat images allows improved visual image quality at high acceleration factors when compared with the water images – especially noticeable, for example, in the 2 mm, 8×8 image.

The 6 estimated motion-parameters (separated into translations and rotations) at each time point for all 6 subjects of the 10-minute scan are shown in Fig 2a. Parameter estimates derived from the full 2 mm, 2×2 accelerated data are shown for both WaterNavs and FatNavs. It can be seen that although the airbag under the subject's head was changed in volume by the same amount for each scan (60 ml) the effect this had on the overall motion was quite variable. Figures 2b and 2c directly compare the parameters from the full-resolution FatNavs against those from the full-resolution WaterNavs (the estimates from the FatNavs have been interpolated to match the timing of the WaterNavs). For both the translations and rotations there is no noticeable bias (bias < 0.02) and very small RMS residuals (0.038 mm and 0.040° - note the smaller range of rotational motion in degrees than translation motion in mm).

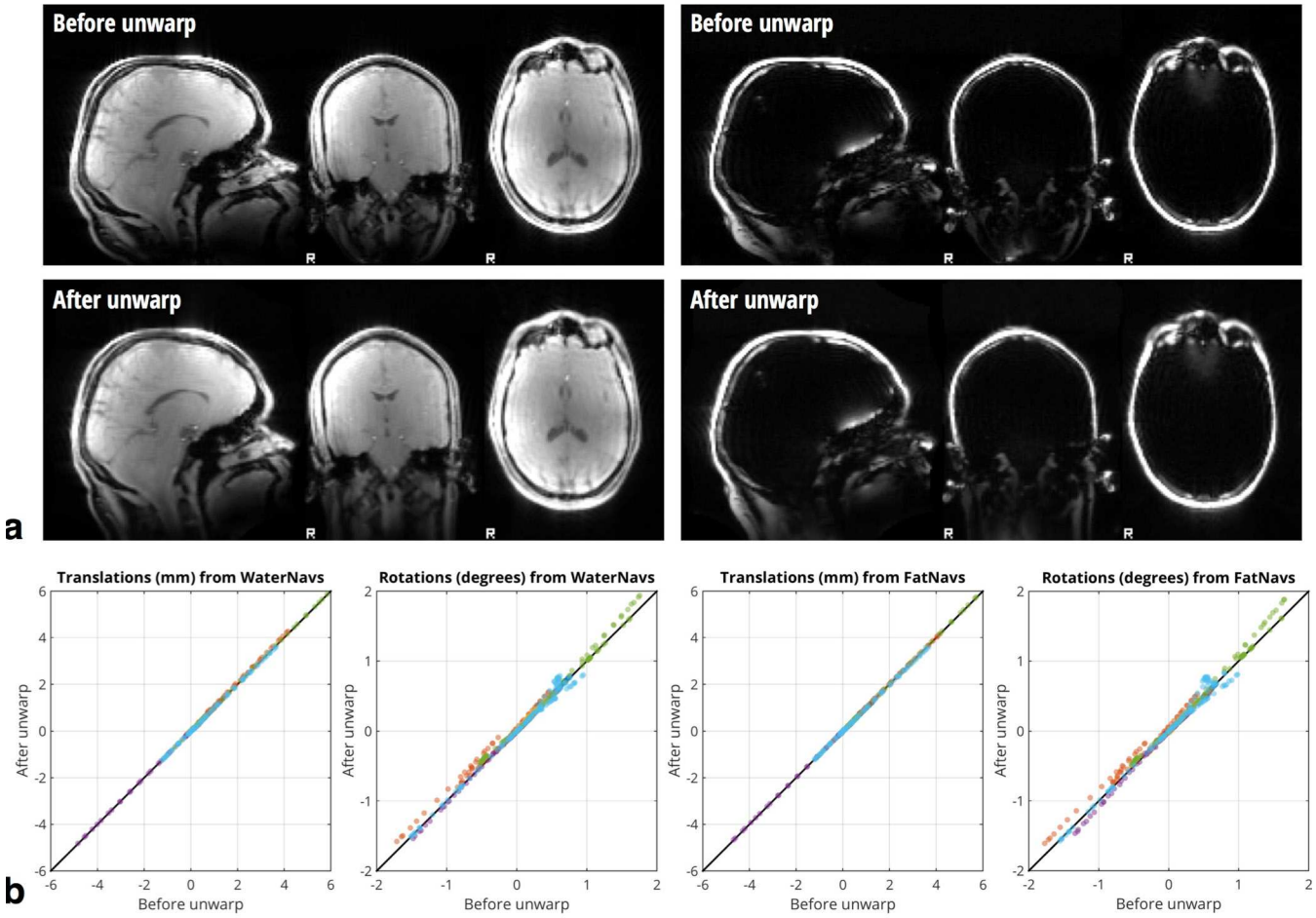

Figure 3: (a) Example orthogonal views of a WaterNav (left) and a FatNav (right) before and after unwarping to correct for gradient non-linearities (2 mm, 2×2 acceleration). (b) Comparison of estimated motion parameters from highest available quality images (2 mm, 2×2 acceleration) before and after unwarping for WaterNavs (left two plots) and FatNavs (right two plots). Note the difference in scale of the plots of translations vs. rotations.

The effect of the unwarping to correct for the gradient non-linearities is shown in Fig. 3, with a visual comparison of both the WaterNavs and the FatNavs before and after correction shown in Fig. 3a. The major difference is in the region of the neck, with small changes also noticeable around the nose and the top of the head. Figure 3b compares the estimated motion parameters from WaterNavs and from FatNavs before and after the unwarping. The estimated translations are not noticeably affected by the unwarping for the WaterNavs or the FatNavs (bias < 0.006 and RMS residuals <0.025 mm) whereas for the estimated rotations there is clearly an effect visible from the figure. The unwarping does not seem to be related to a bias in rotation estimates (bias < 0.005) but there is a non-systematic difference between the estimates before and after application of unwarping which is slightly larger for FatNavs (RMS residuals = 0.058°) than for WaterNavs (RMS residuals = 0.046°).

Figure 4 shows all motion-estimates following unwarping from all 6 subjects for all the combinations of image resolution and acceleration factor tested, compared against the 'true' motion estimates (taken from the original 2 mm, 2×2 accelerated data for the same excitation frequency - either on resonance for water or for fat). It can be observed that the longest duration navigators (top row) all provide strong agreement with the true motion for both the WaterNavs and the FatNavs. For the 2 mm, 12×12 data (bottom left) there is a clear bias in the motion estimates from both the WaterNavs and the FatNavs.

The mean bias and RMS residuals in the motion-estimates across all 6 subjects for each of the combinations of spatial resolution and acceleration factor of the navigators are compared in Fig. 5. For nearly all parameter combinations the bias and RMS residuals are comparable for the FatNavs and the WaterNavs, with FatNavs tending to lead to lower bias and RMS residuals at higher acceleration factors. For the group of parameters corresponding to the longest navigator duration (1.06-1.22 s) the lowest values of bias and RMS residuals are found for both WaterNavs and FatNavs to be the highest resolution data (2 mm). For the shortest navigator duration (144 ms) the bias is very high for the 2 mm resolution images, is lowest around 4-6 mm, and increases again for the 8 mm images. Figure 5(e) shows the combined error scores, which give an approximate indication of the bias and residuals for rotations and translations. Colored dots above bars indicate the parameter sets with lowest combined error for each navigator duration. Overall the combined error scores for WaterNavs and FatNavs are

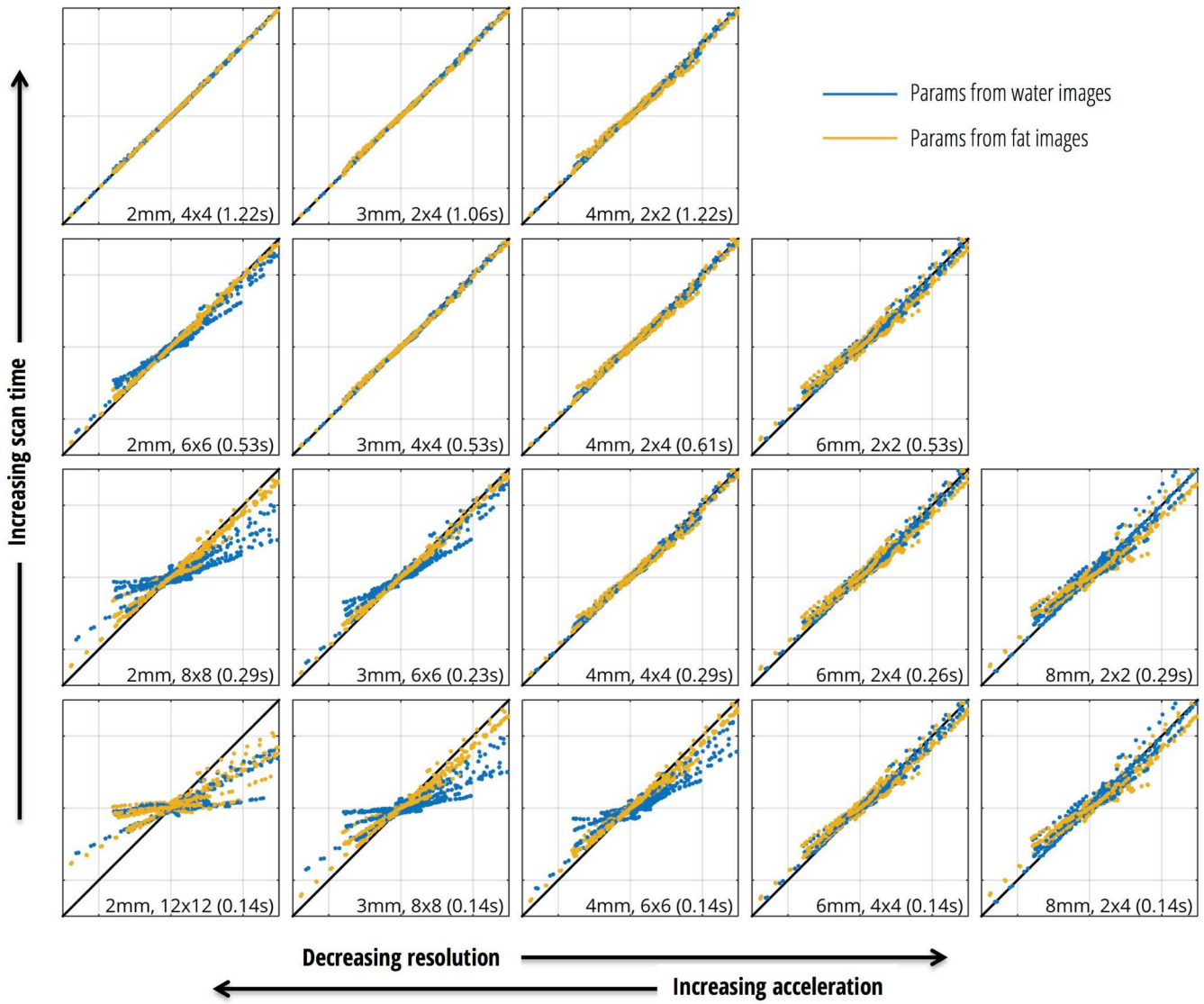

Figure 4: Comparison of motion-estimates derived from retrospectively decimated data to simulate navigator volumes at various spatial resolutions and acceleration factors. All 6 motion parameters appear together on these plots. In all cases the y-axis is used for the motion-estimates from the highest quality estimate available (2 mm, 2×2 acceleration) for the same excitation frequency (either on resonance for water or for fat). All plots are shown with axes covering ± 3.0 mm / ± 3.0°. A line of equality (black) is included on each plot as a reference.

similar – but at very high acceleration factors (6×6 or greater) the FatNavs score noticeably better than WaterNavs

Experiment 2 – Quality of motion-correction using different 3D FatNav resolutions

The estimated motion-parameters using the full 2 mm, 4×4 accelerated 3D FatNavs acquired interleaved with the 10-minute MP2RAGE structural scan are shown in Fig. 6. The motion estimates are also shown estimated from the images resulting from discarding of the data to simulate 3D FatNavs at 3, 4, 6 and 8 mm resolution. Generally, the motion-estimates look quite similar – but the largest disparities are observed for the estimate of the rotational pitch – where, generally, as the voxel size of the 3D FatNavs becomes bigger, the rotational pitch tends to be underestimated. However, it can also be observed that for the estimated rotational pitch during the first few minutes this trend is broken the 4 mm FatNav data, which in this period overestimates the rotation.

Figure 7a shows a zoom from a sagittal section of the full 3D MP2RAGE acquisition at 600 µm before and after retrospective motion-correction using motion estimated from the interleaved 3D FatNavs. The image corrected with the full 2 mm resolution 3D FatNavs still has some minor ringing artifacts, but is a clear improvement over the uncorrected image. By eye there is little perceptible difference between the correction using 2 mm FatNavs or using 3, 4, 6 or 8 mm FatNavs. Careful inspection reveals that some high resolution features (such as the vein marked by the orange arrows) are less well-defined when using 8 mm FatNavs. The difference images shown in Fig. 6b support the observation that when a larger voxel size is used for the 3D FatNavs, the quality of the correction gradually decreases – with the exception of the 6 mm FatNavs, which, for this dataset, perform better than the 4 mm dataset. This result corresponds to the partial overestimation of the rotational pitch by the 4 mm FatNavs observed in Fig. 6.

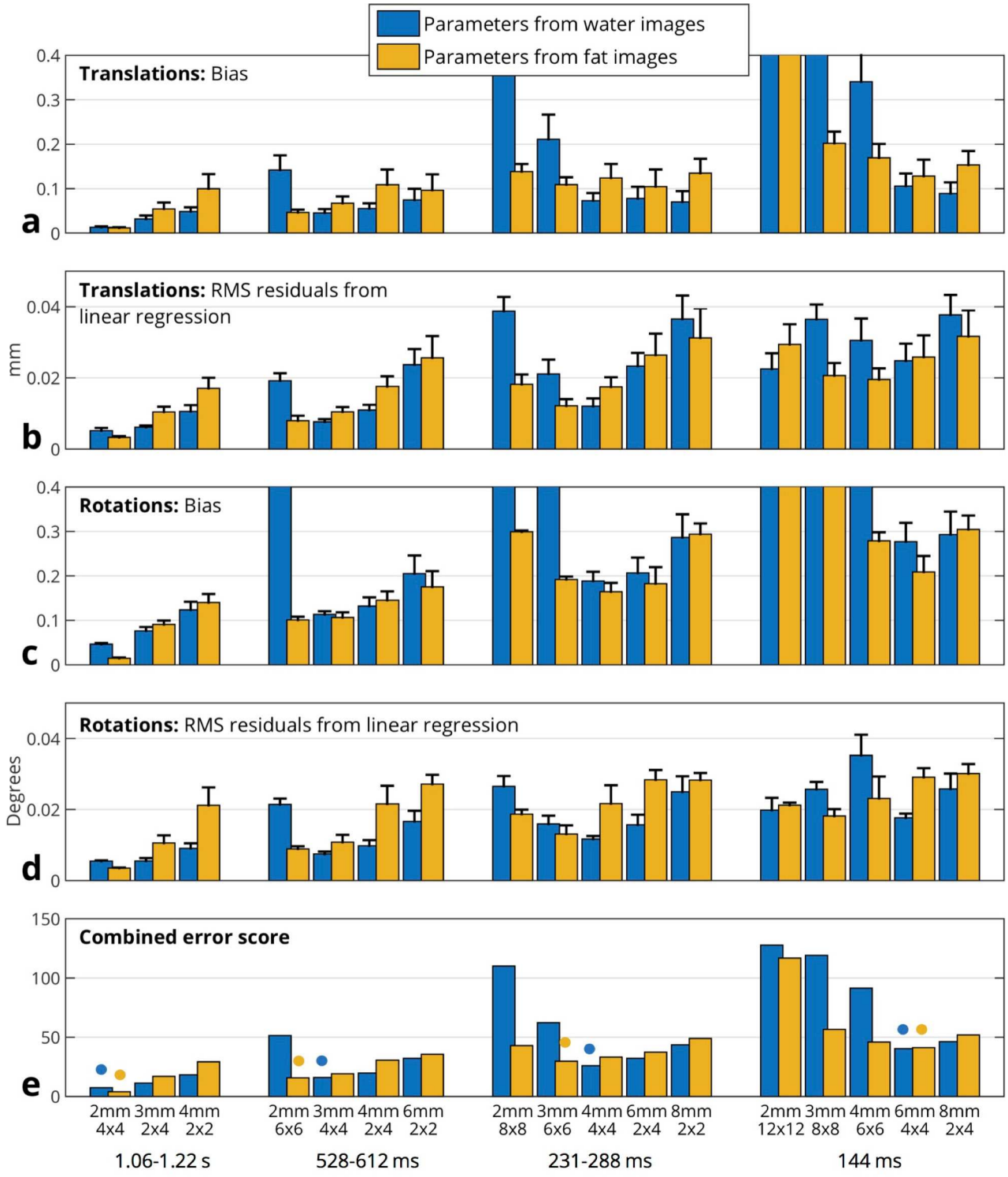

Figure 5: (a-d) Comparison of bias and RMS residuals after linear regression (see text for details of definition used) in the motion-estimates for various combinations of spatial resolution and acceleration factors for the GRE navigators. All bars are the mean across the 6 subjects, with error bars showing the standard error of the mean. Bars are separated into the same 4 groups as the rows in Figs. 1 and 3, whereby each group corresponds to a navigator of approximately the same acquisition time per volume (shortest acquisitions here shown towards the right). **(e)** The combined error score (see text for definition) accounting for bias and residuals across translations and rotations. Colored blue and orange dots indicate the 'optimal' parameter set (lowest error score) for WaterNavs and FatNavs respectively.

Discussion

Optimal parameters for a 3D FatNav

In this work we investigated the effect of the choice of imaging parameters for an image-based motion-navigator on the reliability of the resulting motion parameters – comparing also the differences when a water-based image or a fat-based image is used. We reconfirmed the observation that GRAPPA is able to inherently exploit a sparse image to

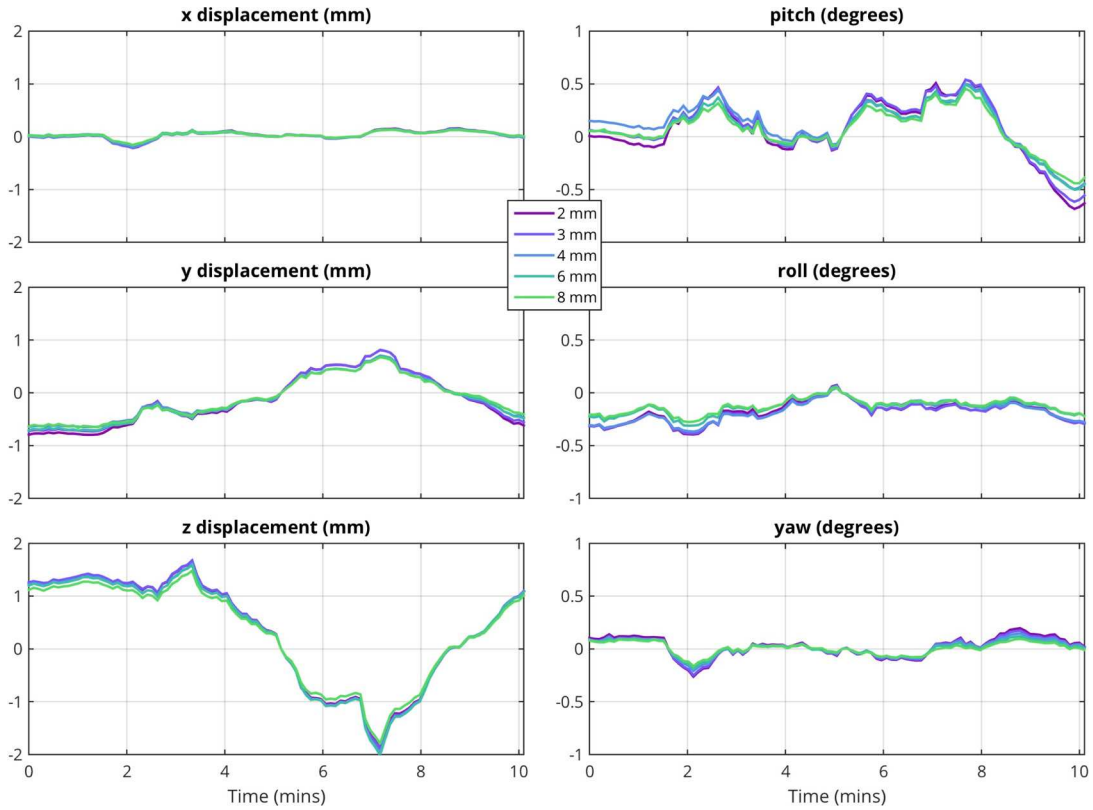

Figure 6: Estimated motion parameters during the 10-minute MP2RAGE structural scan with small deliberate motion of the subject's head. Estimates are shown for the full 2 mm, 4×4 accelerated 3D FatNavs – as well as for estimates from images after discarding data to simulate acquisitions at 3, 4, 6 and 8 mm resolution.

allow very high acceleration factors with acceptable reconstructed image quality. In Fig. 1 the 2 mm, 8×8 images and the 3 mm, 8×8 images for the FatNavs remain visually similar to the images at the same resolution but lower acceleration factors. However, the WaterNavs with the same parameters demonstrate severely compromised image quality. Despite the high visual quality of the reconstructions for the FatNavs at these very high acceleration factors, we were surprised to find that the resulting motion-estimates were not as reliable as the visual image quality might imply. Further investigation is necessary to determine whether the image registration procedure used to generate the motion estimates can be adapted to give more robust motion estimates even at such exceptionally high acceleration factors - where the visual image quality remains high but sufficient artifacts must be arising in the standard processing pipeline to degrade the quality of the motion estimates we obtained.

The levels of bias and RMS residuals which might be considered acceptable for a particular application will depend on the imaging resolution of the host sequence and the magnitude of the expected motion in the studied population group (i.e. differences might be expected between healthy volunteers and patients, or between adults and children), as well as the amount of dead-time in the host sequence (if any) available for the insertion of a navigator acquisition.

Figure 4 provides a visual overview of the main findings of this paper: if there is sufficient time available, the best choice of parameters for the 3D FatNav are 2 mm resolution and 4×4 acceleration. However, as this requires 1.22 s to acquire a single volume, if the sequence has no dead-time, regular insertion of such a navigator would add significantly to the overall scan time. The necessary increase in scan time would, however, depend on how regularly it is necessary to insert the navigator. If, for example, it is found to be sufficient to insert a navigator once every 10 s, then using the optimal navigator parameter set would only add around 12% to the overall scan time. However, if it is decided that some compromises can be made in terms of bias and RMS residuals in the motion estimates then it may be sufficient to use the 4 mm, 6×6 accelerated 3D FatNav which would take only 144 ms. Sampling once every 10 s would add less than 2% to the overall scan time.

Influence of unwarping correction for gradient non-linearities

As demonstrated by Fig. 3, the unwarping has only a very small influence on the estimated motion-parameters – and the effect is very similar for the WaterNavs and the FatNavs. We had speculated that the FatNavs may be more affected by the application of unwarping as the fat signal is primarily located further from the scanner isocenter meaning a greater proportion of the signal is in strongly warped regions. However, it is difficult to determine which image features have the strongest influence on the quality of the alignment, and our results suggest that the WaterNavs and FatNavs are affected in a similar way within the range of movement we measured – and for our gradient coil. We do not currently have an independent measure of the head-motion to determine whether the estimates are closer to the actual motion of the head following the unwarping – but it can be observed from the images that the unwarped volumes are a better representation of the true

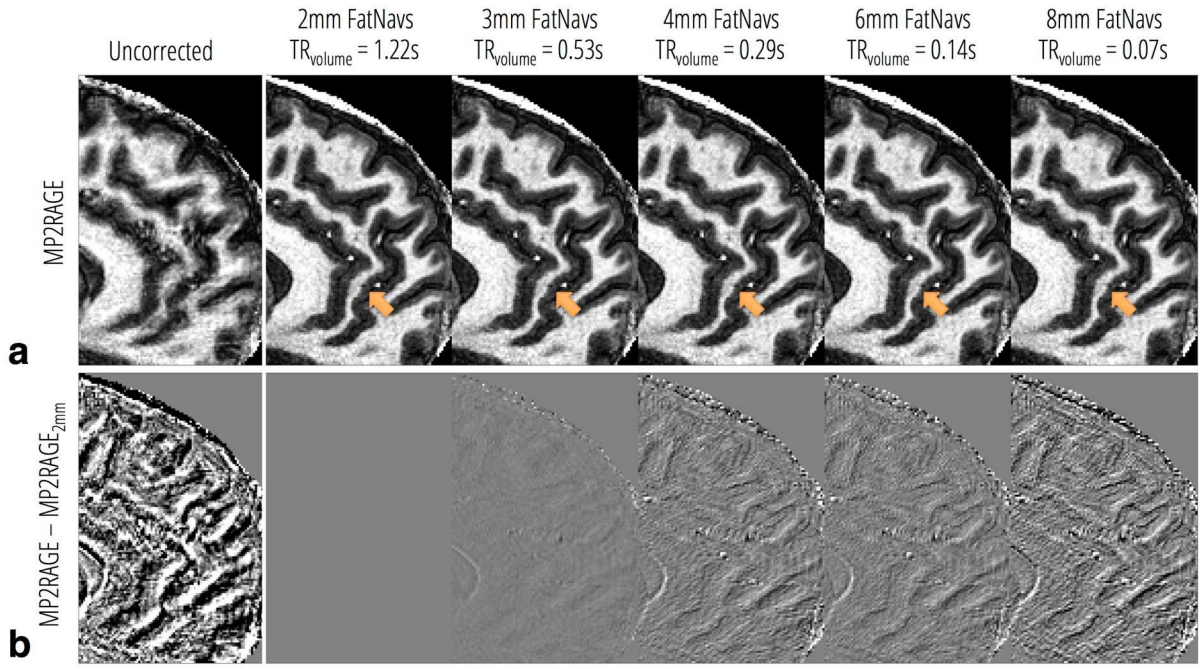

Figure 7: (a) Visual comparison of the quality of a zoomed sagittal section from the 600 μm isotropic MP2RAGE dataset (which was corrupted by small deliberate head motion) after application of motion-correction using the full 2 mm resolution of the 3D FatNavs and using 3D FatNavs with data discarded to simulate navigator resolutions of 3, 4, 6 and 8 mm. Arrows highlight a dark vein where some variation in image sharpness is observable by eye. The original corrupted image without motion-correction is shown on the far left. (b) Difference between image shown on the top row and the best corrected image (using 2 mm 3D FatNavs).

head anatomy, so we expect the unwarping to have made the estimates more accurate. The difference in estimates is so small, however, that it is unlikely to have a noticeable effect on the motion-corrected image. We would expect this result to also on other systems incorporating head-only gradient sets, as these smaller coils necessarily have a smaller region of high linearity. We would also expect that the influence of unwarping would be even smaller on systems using whole-body gradient sets.

Comparison of WaterNavs and FatNavs

Both the bias and RMS residuals of the motion estimates from the FatNavs were found to be comparable to those of the WaterNavs for nearly all combinations of spatial resolution and acceleration factor of the navigator (see Fig. 4). At very high acceleration factors (6×6 or greater) the parameters from the FatNavs have noticeably lower combined error scores than the WaterNavs.

FatNavs also have the advantage over WaterNavs that they have minimal impact on the magnetization of the water spins being probed by the host sequence. However, despite these advantages, the question also arises as to whether the motion-parameters obtained from a fat image are as good a measure of the real motion of the head as those obtained from a water image (for the plots in Fig. 3 the comparison was always performed against a reference with the matched excitation frequency). To test whether the WaterNavs and the FatNavs are measuring the 'same' motion, we took the original 2 mm, 2×2 accelerated data (which we used as the 'reference' motion for Figs. 3 and 4) and plotted the motion estimates from the FatNavs against those from the interleaved WaterNav acquisitions, shown in Figs. 2b and 2c. For both the translations and rotations there is a strong correlation and little noticeable bias between the estimates from WaterNavs vs FatNavs. By eye there appears to be more noise (RMS residuals) in the comparison of rotation estimates, a trend which is supported by a very small difference in the RMS residuals metric (0.038 mm vs 0.040°), but the difference clearly visible by eye is largely explained by the fact that the head-motion induced by the inflating/deflating air bag involved more translational than rotation motion, and the axes for the rotations plot are smaller than for the translations.

With the general shape of the scalp (which dominates the fat image) being, to a first approximation, similar to a sphere – there is the possibility that the fat image is inherently less sensitive to rotations than the water image. Figure 2c suggests that the fat layer is sufficiently different from a sphere to provide reliable estimates of head rotation. We must also consider that the fat layer within the head is not completely rigidly fixed to the skull – although our initial experience through visual comparison of co-registered fat images from different head poses in a number of subjects suggests that this only becomes a problem around the back of the neck for subjects with a high body mass index. Being a small proportion of the field of view, we would not expect this to have a large effect on the motion-estimation – but further study would be required to ensure the robustness of the fat-derived motion estimates for all subject body-types.

It should be noted that the results presented in Figs. 2b and 2c are less directly interpretable for very small motion

(~≤0.2 mm and ~≤0.2°). This is because the motion estimates from the FatNavs were temporally interpolated to coincide with the timing of the WaterNav acquisitions. This means that for slow drifting motion the values should be directly comparable, but for faster motion – that might result from breathing-related motion, or swallowing – the two acquisitions did not measure the head in precisely the same pose. For an application where the very highest quality of motion-estimate is required, it may therefore be useful to perform an experiment where motion-estimates are compared against an independent gold standard, such as using a mouth-piece mounted marker and camera setup. As evidenced by the quality of the motion-correction shown in Fig. 7 (compare 'uncorrected' vs. '2 mm FatNavs'), however, the potential for further improvement may prove minimal, as with the current implementation of the MP2RAGE scan timing, a FatNav is acquired only once every 6 seconds, meaning that 'fast' motion will not be adequately sampled. Rather than attempting to get the very highest quality motion estimates from a single FatNav acquired once every 6 seconds, it may therefore be more appropriate to attempt alter the sequence timing such that an additional faster, lower resolution FatNav is also acquired in between the two readout trains for the MP2RAGE scan in order to better sample the faster movements.

Varying resolution of FatNav used for motion-correction

In Experiment 1 we examined the loss of accuracy and precision associated with acquiring shorter navigator volumes. However, the critical question for application of the method is how much of an influence these choices really have on the quality of the motion-corrected images. Unfortunately this is a very difficult question to address, as no two scans will have the same motion profile – and therefore the artifacts will also manifest themselves differently. To give a rough visual indication of the differences, we performed Experiment 2, where a subject made slow, small deliberate movements during a 10-minute structural MP2RAGE scan. It is clear from the motion-parameters shown in Fig. 5 that the dominant translation was in the z-direction – and the dominant rotation axis was pitch. As the voxel size for the FatNav was artificially reduced, so the motion parameters became less reliable. This is most evident visually from the rotations along the pitch axis (top-right in Fig. 5) where the curve for 8 mm FatNavs deviates noticeably from the original from the 2 mm FatNav data. We also made the unexpected observation for this dataset that the 4 mm FatNavs led to *overestimates* of pitch rotation, deviating from the trend of underestimation of motion parameters with larger navigator voxel-sizes. We were unable to identify the cause of this behaviour, and as we did not observe the same effect in the 6 subjects used for Experiment 1 we consider it to be an outlier. Given that the maximal overestimation was small (< 200 μm) and did not lead to clear differences visible by eye in the corrected images, we do not consider finding the cause of this anomaly to be a priority at this time.

The effect of the FatNav resolution on the motion-corrected structural image is shown in Fig. 7, where the correction using the original 2 mm FatNavs is a clear improvement over the uncorrected image. There is some small remaining ringing artifact, which we attribute to the fact that the FatNavs are acquired only once every 6 seconds, and therefore cannot be expected to provide perfect correction. By eye there is very little appreciable difference between using the 2 mm FatNavs or using 3, 4, 6 or 8 mm FatNavs – but careful inspection reveals there is a slight loss of sharpness in some of the smallest vessels. For this experiment it was not possible to retrospectively decrease the acceleration factor of the original FatNav data (4×4), which leads to a very small acquired matrix size for the 8 mm data (only 4×6=24 readout lines for the whole 3D volume).

Retrospective motion-correction in combination with GRAPPA

We would like to emphasize the important finding that retrospective motion-correction applied in k-space can very easily be adapted so that it is compatible with parallel acceleration of the main 3D sequence using GRAPPA. As the k-space samples following retrospective motion-correction no longer conform to a Cartesian grid it is not obvious that Cartesian GRAPPA can still be used effectively. Encouraged by the recent results of Loktyushin et al (20) where motion-parameters were successfully estimated directly from accelerated k-space data, we tested the simple method demonstrated in this work: first apply GRAPPA as normal to motion-corrupted data, then interpolate estimated translations and rotations from 3D FatNavs to give pseudo-motion estimates for the non-acquired lines of data. As long as the motion remains small enough such that there is no significant motion-related parallel imaging artefact in the original images then we would expect this simple method will give good results. To be able to perform good correction in the presence of larger motion it may be necessary to develop an iterative algorithm whereby the weights for GRAPPA reconstruction can be re-estimated alongside the application of the motion-correction (20).

Further considerations

The aim of the current work was to investigate the reliability of motion-estimates from different navigator acquisitions for the tracking of small motion of compliant subjects. Some patient populations, such as children, may be particularly susceptible to much larger motion. We would expect that FatNavs could also be used to track such motion – but depending on the details of the motion profile it may lead to increased residual artifacts in the motion-corrected image due to the increase in 'gaps' and overlapping regions of the corrected k-space. Such artifacts could be mitigated by implementing a sufficiently fast image reconstruction pipeline for the navigators to allow real-time updates of the scanner coordinates (i.e. 'prospective' motion correction). Alternatively, iterative methods should also be capable of compensating for gaps in k-space by making use of RF coil sensitivity information in a similar way to parallel imaging techniques (21).

All of the results we present in this work are dependent on the choice of algorithm used to estimate the motion-parameters from the images – as well as the image reconstruction algorithm used to reconstruct each navigator. We chose to use the *realign* tool from SPM for the image co-

registration, as our initial testing suggested that it is particularly suited to handling sub-voxel shifts in a robust fashion. If applications are found where it would be especially relevant to be able to match the low bias and RMS residuals associated with the slowest FatNav – but in a shorter acquisition time – then it may be necessary to investigate alternative approaches to the registration which are specifically adapted to the contrast and signal distribution in fat images. It may be beneficial, for example, to incorporate the prior knowledge of the signal distribution (perhaps obtained from the GRAPPA calibration volume acquired at the start of the scan) to directly estimate the motion-parameters as part of the FatNav image reconstruction process from the raw k-space data.

Conclusion

We tested the bias and RMS residuals associated with motion-estimates derived from 3D FatNav data acquired at various spatial resolutions and acceleration factors and conclude that if there is time available, the 2 mm, 4×4 accelerated acquisition, taking 1.22 s, is able to give motion estimates virtually indistinguishable from the highest quality data tested (2 mm, 2×2 accelerated). If the FatNav needs to be shorter for a particular application, then good accuracy and precision can still be achieved with a 144 ms navigator – where it was found that a lower resolution navigator (4 mm, 6×6 acceleration) avoids the additional bias observed when using exceptionally high acceleration factors (8×8 or higher). Direct comparison between motion-estimates from FatNavs and WaterNavs showed very good agreement, and they demonstrated similar performance for different choices of resolution and acceleration – with FatNavs giving lower error scores than WaterNavs at very high acceleration factors.

Acknowledgments

This work was in part supported by the Centre d'Imagerie BioMédicale (CIBM) of the EPFL, UNIL, UNIGE, HUG, CHUV and the Leenards and Jeantet Foundations, as well as SNSF project number 205321_153564.

References

1. Ooi MB, Krueger S, Thomas WJ, Swaminathan S V, Brown TR. Prospective real-time correction for arbitrary head motion using active markers. Magn Reson Med 2009;62:943–54. doi: 10.1002/mrm.22082

2. Zaitsev M, Dold C, Sakas G, Hennig J, Speck O. Magnetic resonance imaging of freely moving objects: prospective real-time motion correction using an external optical motion tracking system. Neuroimage 2006;31:1038–50. doi: 10.1016/j.neuroimage.2006.01.039.

3. Qin L, van Gelderen P, Derbyshire JA, Jin F, Lee J, de Zwart JA, Tao Y, Duyn JH. Prospective head-movement correction for high-resolution MRI using an in-bore optical tracking system. Magn Reson Med 2009;62:924–34. doi: 10.1002/mrm.22076.

4. Schulz J, Siegert T, Reimer E, Labadie C, Maclaren J, Herbst M, Zaitsev M, Turner R. An embedded optical tracking system for motion-corrected magnetic resonance imaging at 7T. Magn Reson Mater Phy 2012;25:443–53. doi: 10.1007/s10334-012-0320-0.

5. Maclaren J, Armstrong BSR, Barrows RT, et al. Measurement and Correction of Microscopic Head Motion during Magnetic Resonance Imaging of the Brain. PLoS One 2012;7:e48088. doi: 10.1371/journal.pone.0048088.

6. Welch E, Manduca A. Spherical navigator echoes for full 3D rigid body motion measurement in MRI. Magn Reson Med 2001;41:32–41. doi: 10.1002/mrm.10012.

7. White N, Roddey C, Shankaranarayanan A, Han E, Rettmann D, Santos J, Kuperman J, Dale A. PROMO: Real-time prospective motion correction in MRI using image-based tracking. Magn Reson Med 2010;63:91–105. doi: 10.1002/mrm.22176.

8. Tisdall MD, Hess AT, Reuter M, Meintjes EM, Fischl B, van der Kouwe AJW. Volumetric navigators for prospective motion correction and selective reacquisition in neuroanatomical MRI. Magn Reson Med 2012;68:389–99. doi: 10.1002/mrm.23228.

9. Van der Kouwe AJW, Benner T, Dale AM. Real-time rigid body motion correction and shimming using cloverleaf navigators. Magn Reson Med 2006;56:1019–32. doi: 10.1002/mrm.21038.

10. Tisdall MD, Polimeni JR, van der Kouwe AJW. Motion-corrected 350 μm isotropic MPRAGE at 3 T using volumetric navigators (vNavs). In: Proceedings of the 21st Annual Meeting of the International Society of Magnetic Resonance in Medicine, Salt Lake City, USA. Vol. 33. ; 2013. p. 268.

11. Pipe JG. Motion correction with PROPELLER MRI: application to head motion and free-breathing cardiac imaging. Magn Reson Med 1999;42:963–9.

12. Anderson AG, Velikina J, Block W, Wieben O, Samsonov A. Adaptive retrospective correction of motion artifacts in cranial MRI with multicoil three-dimensional radial acquisitions. Magn Reson Med 2013;69:1094–103. doi: 10.1002/mrm.24348.

13. Atkinson D, Hill DLG, Stoyle PNR, Summers PE, Clare S, Bowtell R, Keevil SF. Automatic compensation of motion artifacts in MRI. Magn Reson Med 1999;41:163–170.

14. Gallichan D, Marques JP, Gruetter R. Retrospective correction of involuntary microscopic head-movement using highly-accelerated fat image-navigators (3D FatNavs) at 7T. Magn Reson Med (Early View online) 2015.

15. Griswold MA, Jakob PM, Heidemann RM, Nittka M, Jellus V, Wang J, Kiefer B, Haase A. Generalized autocalibrating partially parallel acquisitions (GRAPPA). Magn Reson Med 2002;47:1202–1210. doi: 10.1002/mrm.10171.

16. Maclaren J, Speck O, Stucht D, Schulze P, Hennig J, Zaitsev M. Navigator accuracy requirements for prospective motion correction. Magn Reson Med 2010;63:162–70. doi: 10.1002/mrm.22191.

17. Marques JP, Kober T, Krueger G, van der Zwaag W, Van de Moortele P-F, Gruetter R. MP2RAGE, a self bias-field corrected sequence for improved segmentation and T1-mapping at high field. Neuroimage 2010;49:1271–81. doi: 10.1016/j.neuroimage.2009.10.002.

18. Fessler J, Sutton B. Nonuniform fast Fourier transforms using min-max interpolation. IEEE Trans. Signal Process. 2003;51:560–574.

19. Skare S, Hartwig A, Mårtensson M, Avventi E, Engström M. Properties of a 2D fat navigator for prospective image domain correction of nodding motion in brain MRI. Magn Reson Med 2015;73:1110–1119. doi: 10.1002/mrm.25234.

20. Loktyushin A, Babayeva M, Gallichan D, Krueger G, Scheffler K, Kober T. Retrospective rigid motion correction of undersampled MRI data. In: Proceedings of the 23rd Annual Meeting of the ISMRM, Toronto, Canada. ; 2015. p. 2556.

21. Bammer R, Aksoy M, Liu C. Augmented generalized SENSE reconstruction to correct for rigid body motion. Magn Reson Med 2007;57:90–102. doi: 10.1002/mrm.21106.